JAM CM Journal of Applied Mathematics and Computational Mechanics 2022, 21(4), 73-85
www.amcm.pcz.pl p-ISSN 2299-9965
DOI: 10.17512/jamcm.2022.4.07 e-ISSN 2353-0588

THE IMPACT OF VARIABLE FLUID PROPERTIES ON NATURAL CONVECTION FLOW PAST A VERTICAL CONE

Darbhasayanam Srinivasacharya, Bhanoth Rajender

Department of Mathematics, National Institute of Technology
Warangal, TS, India
dsc@nitw.ac.in, rajender.nitw@gmail.com

Received: 20 June 2022; Accepted: 2 October 2022

Abstract. A free convective flow of an incompressible viscous fluid past an isothermal vertical cone is investigated with variable viscosity and variable thermal conductivity. The constant wall temperature (CWT) and constant wall heat flux (CHF) conditions are used as temperature boundary conditions at the surface of the cone. The successive linearization method is applied to linearize the governing nonlinear differential equations of the flow. The numerical solution for the resulting linear equations is attained through the Chebyshev spectral collocation method. The impact of significant parameters on the velocity and temperature, in addition to heat and mass transfer rates, is evaluated and represented graphically for the CWT and CHF situations. The local heat transfer rate decreases, and the coefficient of the skin friction increases with an increase in the viscosity and thermal conductivity parameters for CWT conditions, but the reverse trend is noticed for CHF conditions.

MSC 2010: *76D10, 76M22*
Keywords: *viscous fluid, vertical isothermal cone, successive linearization, Chebyshev collocation method*

1. Introduction

The convective heat transfer from different geometries (including plates, wedges, and cylinders) has attracted a lot of attention in recent decades, both theoretically and experimentally, because of their wide range of applications in a wider range of engineering processes, fiber technology, nuclear cooling systems, surface treatment, high-speed thermal aerodynamics, polymer engineering, spray deposition methods, etc. In particular, the flow past a vertical cone has attracted much attention due to its vast application in industrial and engineering processes. For example, the cone penetration test is a standard quality control procedure for measuring the rheological properties of soils, soft solids encountered in food, and personal care products. For the flow over a vertical cone under steady conditions, several authors developed

similarity solutions. Merk and Prins [1] proposed a solution for free convective flow across an isothermal cone based on similarity transformations. Hering and Grosh [2] investigated a similarity solution for a non-isothermal right circular cone. Kafoussias [3] scrutinized the consequence of mass transfer on the flow of a viscous fluid past a vertical cone with free convection. Using similarity analysis, Ece [4] explored the impact of a magnetic field on a laminar natural convection flow past a vertical cone by applying mixed thermal boundary conditions. Palani and Raghavan [5] examined the simultaneous impact of the transverse magnetic field, buoyancy, and chemical reaction on the natural convection heat and mass transfer past an isothermal vertical cone. Vanitha and Kumar [6] analyzed the effect of the magnetic field on the transient free convective flow past a vertical cone. Ajay and Srinivasa [7] considered the MHD natural convective flow over a truncated cone. Kannan et al. [8] considered the impact of heat source/sink on the natural convective MHD flow from a cone with variable surface heat flux.

The properties of fluids, for example, viscosity and thermal conductivity, are well known to change with the temperature. Kays and Crawford [9] provided a variety of relationships between fluid physical properties and temperature. The intensification in temperature speeds up the transport phenomena by decreasing viscosity all over the temperature boundary layer, which influences the heat transfer rate. The enhancement in temperature in lubricating fluids generates internal friction, which modifies the viscosity of the fluid, which will no longer remain constant. Herwig and Gersten [10] were the first to examine the influence of variable fluid properties on laminar boundary layer flow. Since then, a number of researchers have been examining the effect of variable thermal conductivity and viscosity on flow, heat transfer, and mass transfer in a variety of physical configurations. Several studies have introduced temperature dependent properties and reported significant influence of these properties over the flow characteristics. Furthermore, it is clear that adequate studies are not available to study the effect of temperature dependent viscosity and thermal conductivity on a free convection flow of a viscous incompressible fluid along an isothermal vertical cone. This has motivated the present study. Chand et al. [11] studied the effects of variable gravity on thermal instability in a horizontal layer of a nanofluid in an anisotropic porous medium. Choudhury and Hazarika [12] discussed the significance of variable thermal conductivity and viscosity on free convective flow across a vertical plate under slip flow conditions with periodic plate temperature. Mekheimer and Abd Elmaboud [13] discussed the effect of variable fluid properties on the peristaltic flow in a vertical asymmetric channel. Anjali Devi and Prakash [14] examined the hydromagnetic flow over a slandering stretching sheet by taking viscosity and thermal conductivity as functions of temperature. Umavathi et al. [15] researched the free convection viscous fluid flow between vertical parallel plates with the impact of varying viscosity and thermal conductivity. Srinivasacharya and Jagadeeshwar [16] investigated viscous fluid flow across an exponential stretching sheet on the presumption that thermal conductivity and viscosity vary linearly with temperature. Mushtaq et al. [17] analyzed the variable fluid properties and their

influences on MHD flow due to the exponentially stretching sheet. Ahmed et al. [18] numerically investigated the outcome of variable viscosity and thermal conductivity on MHD convective flow past a non-isothermal moving vertical plate. Ahmed et al. [19] explored the impact of an exothermic catalytic chemical reaction on the free convection flow of a viscous fluid past a curved surface where the thermal conductivity and viscosity are proportional to the temperature. Chu et al. [20] developed a mathematical model to scrutinize the two-dimensional magnetohydrodynamic boundary layer flow of second grade nanofluid toward a permeable and stretchable Riga plate surface with variable thermal conductivity and variable mass diffusivity. Khan et al. [21] addressed the effects of temperature dependent viscosity and thermal conductivity on the bioconvection flow in non-Newtonian nanofluid over a periodically moving surface. Song et al. [22] communicated the thermal assessment of Sutterby nanofluid containing the gyrotactic microorganisms over an axially stretched cylinder with melting heat transfer and variable thermal features. Salahuddin et al. [23] inspected the heat and mass transfer along with induced magnetic field in an incompressible Williamson fluid with variable thermo-physical properties. Islam et al. [24] considered the natural convection within a prismatic cavity filled with Cu-H_2O nanofluid for visualizing heat transport characteristics through the heat line method with two different temperature boundary conditions. Sarkar and Alam [25] explored the role of variable viscosity and thermal conductivity on natural convective flow past a vertical plate with magnetic and heat conduction effects. Hasan et al. [26] studied the impact of temperature-dependent viscosity on free convective flow past a vertical impervious circular cone with constant heat flux.

The current investigation emphasizes the study of an incompressible viscous fluid flow along a vertical cone with variable thermal conductivity and viscosity. The novelty of the work is to develop a similarity solution for the free convection flow past a vertical cone with constant temperature and flux at the surface along with variable thermal conductivity and viscosity, using successive linearization to linearize the governing equations and then solve the resulting equations by the pseudo-spectral approach. This successive linearization followed by the Chebyshev spectral technique was applied to solve the convection heat transfer and mass transfer problems. The influences of different geometry and flow factors on the velocity component, temperature, and heat transfer rate are thoroughly examined.

2. Formulation of the problem

Consider an incompressible, steady-state and laminar flow of Newtonian fluid along a vertical down-pointing cone with local radius r and half-angle ϕ. Choose a coordinate system in which the origin is taken as the apex of the cone, the x-axis runs along the cone's surface, and the y-axis is upright to it, as depicted schematically in Figure 1. The local radius at a point located and the radius of a cone can be guesstimated by $r = x\sin(\phi)$ [4]. The ambient temperature is assumed as T_∞.

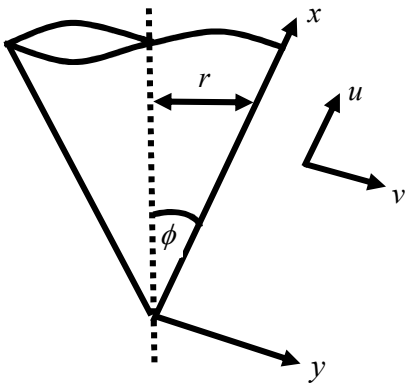

Fig. 1. Geometry and coordinate system

Applying Boussinesq approximation and utilizing the boundary layer concepts, the equations describing the flow are:

$$\frac{\partial}{\partial x}(ur) + \frac{\partial}{\partial y}(vr) = 0 \tag{1}$$

$$\rho\left(u\frac{\partial u}{\partial x} + v\frac{\partial u}{\partial y}\right) = \frac{\partial}{\partial y}\left(\mu\frac{\partial u}{\partial y}\right) + \rho\,(T - T_\infty)g\beta\cos(\phi) \tag{2}$$

$$u\frac{\partial T}{\partial x} + v\frac{\partial T}{\partial y} = \frac{1}{\rho C_p}\frac{\partial}{\partial y}\left(k\frac{\partial T}{\partial y}\right) \tag{3}$$

where u, v, 0 signify the velocity vector, T denotes the temperature of the fluid, g denotes the gravitational acceleration, μ represents the variable viscosity, ρ represents the fluid density, β denotes the thermal expansion coefficient, C_p denotes the specific heat, and k denotes the variable thermal conductivity of the fluid.

The viscosity and thermal conductivity are considered to be linearly dependent on the temperature [21] and are given by

$$\mu = \mu_\infty[1 + \lambda\,(T_\infty - T)] \text{ and } k = k_0[1 + \gamma(T - T_\infty)]. \tag{4}$$

where μ_∞ and k_0 represent the absolute viscosity and the thermal conductivity of the fluid, respectively, and λ and γ are constants.

No-slip at the surface of the cone and no stream condition in the ambient medium are the associated conditions on the boundary for the flow configuration. These are expressed as

$$u = 0, v = 0, \text{ at } y = 0 \text{ and } u \to 0, \text{ as } y \to \infty \tag{5}$$

In addition, for the temperature on the surface of the cone, one can either have constant temperature T_w (CWT) or a constant heat flux q_w (CHF). Thus, the conditions for the temperature on the boundary are written as

Type – I (CWT): $T = T_w$ at $y = 0$ (6)

Type – II (CHF): $k\frac{\partial T}{\partial y} = q_w$ at $y = 0$ (7)

and far-off from the cone, the temperature of the free stream is constant i.e. $T \to T_\infty$, as $y \to \infty$.

The stream function is defined in the context of equation (1) as $u = -\frac{1}{r}\frac{\partial \psi}{\partial z}$ and $w = \frac{1}{r}\frac{\partial \psi}{\partial r}$.

For type – I boundary conditions, we define the following similarity transformations

$$\xi = \frac{x}{L},\ \eta = \frac{y}{L}\left(\frac{Gr}{\xi}\right)^{\frac{1}{4}},\ \Psi = r\,\nu\,Gr^{\frac{1}{4}}\,\xi^{\frac{3}{4}} f(\eta),\ T = T_\infty + (T_w - T_\infty)\theta(\eta) \quad (8)$$

For type – II boundary conditions, the similarity transformations are given by

$$\xi = \frac{x}{L},\ \eta = \frac{y}{L}\left(\frac{Gr}{\xi}\right)^{\frac{1}{5}},\ T = T_\infty + \frac{q_w L}{k}\,Gr^{-\frac{1}{5}}\,\xi^{\frac{1}{5}}\theta(\eta),\ \psi = r\nu Gr^{\frac{1}{5}}\xi^{\frac{4}{5}} f(\eta) \quad (9)$$

where $Gr = \frac{L^3 g\beta\cos\phi(T_w - T_\infty)}{\upsilon^2}$ is the Greshof number and L is the typical length.

Applying the similarity transformations (8) and (9) in the Eqs. (2) and (3), we get the non-dimensional equations shown below:

– For type – I boundary conditions:

$$(1+A)f''' - A\theta f''' - A\theta' f'' + \frac{7}{4}ff'' - \frac{1}{2}f'^2 + \theta = 0 \quad (10)$$

$$\frac{1}{\mathrm{Pr}}\theta'' + \frac{\in}{\mathrm{Pr}}(\theta\theta'') + \frac{\in}{\mathrm{Pr}}(\theta')^2 + \frac{7}{4}f\theta' = 0 \quad (11)$$

– For type – II boundary conditions

$$(1+A)f''' + \frac{9}{5}ff'' - \frac{3}{5}f'^2 - A\theta' f'' - A\theta f''' + \theta = 0 \quad (12)$$

$$\frac{1}{\mathrm{Pr}}\theta'' + \frac{\in}{\mathrm{Pr}}\theta\theta'' + \frac{1}{\mathrm{Pr}}\in \theta'^2 - \frac{1}{5}f'\theta + \frac{9}{5}f\theta' = 0 \quad (13)$$

where $\mathrm{Pr} = \frac{\upsilon}{\alpha_0}$ denotes the Prandtl number, A denotes the viscosity parameter, and $\in$ denotes the thermal conductivity parameter.

The dimensionless form of conditions on the boundary is

$$f(\eta) = 0, f'(\eta) = 0, \theta(\eta) = 1,\ \text{at}\ \eta = 0\ \text{and}$$
$$f'(\eta) = 0, \theta(\eta) = 0\ \text{as}\ \eta \to \infty\ \text{for CWT case} \quad (14)$$

and

$$f(\eta) = 0, f'(\eta) = 0, \theta'(\eta) = -1,\ \text{at}\ \eta = 0\ \text{and}$$
$$f'(\eta) = 0, \theta(\eta) = 0\ \text{as}\ \eta \to \infty\ \text{for CHF case} \quad (15)$$

The most important findings of practical significance are the local skin-friction coefficient and local rate of heat transfer in terms of Nusselt number. The dimensionless representation of skin-friction coefficient C_f and Nusselt number (Nu) for CWT boundary conditions are

$$C_f^I = Gr^{\frac{3}{4}}\,\xi^{\frac{3}{4}}\,f''(0) \text{ and } Nu^I = -Gr^{\frac{1}{4}}\,\xi^{-\frac{1}{4}}\,\theta'(0) \tag{16}$$

and for CHF boundary conditions are

$$C_f^{II} = Gr^{\frac{3}{5}}\,\xi^{\frac{2}{5}}\,f''(0) \text{ and } Nu^{II} = \frac{1}{\theta(0)}\,Gr^{\frac{1}{5}}\,\xi^{\frac{4}{5}} \tag{17}$$

3. Methodology

The set of differential equations (10)-(11) and (12)-(13) are linearized by employing a successive linearization method (SLM) [22]. The solutions of the ensuing linearized equations are attained by employing the Chebyshev spectral method [23]. Using SLM, unknown functions $f(\eta)$ and $\theta(\eta)$ are taken as

$$f(\eta) = f_i(\eta) + \sum_{m=0}^{i-1} f_m(\eta),\ \theta(\eta) = \theta_i(\eta) + \sum_{m=0}^{i-1} \theta_m(\eta) \tag{18}$$

where $f_i(\eta)$ and $\theta_i(\eta)$ (i = 1, 2, ...) are the function to be determined and $f_m(\eta)$ and $\theta_m(\eta)$ ($m \geq 1$) are guesstimates that can be determined by repeatedly solving the linear terms of the set of equations obtained by employing Eq. (18) in the Eqs. (10)-(11) and (12)-(13). The underlying idea of the SLM is that f_i and θ_i are quite small even as i turns out to be large, so nonlinear terms in f_i and θ_i and their derivatives are reasoned to be infinitesimal and thus ignored.

The preliminary guesses $f_0(\eta)$ and $\theta_0(\eta)$ are selected to match the conditions on the boundary (14) and (15). The iterative solutions f_i and θ_i are attained by recursively solving the following linearized equations for CWT boundary conditions

$$a_1\,f_i''' + a_2 f_i'' + a_3 f_i' + a_4 f_i + a_5\,\theta_i' + a_5\,\theta_i = a_7 \tag{19}$$

$$b_1 f_i + b_2 \theta_i'' + b_3 \theta_i' + b_4 \theta_i = b_5 \tag{20}$$

The linearized equations for CHF boundary conditions are

$$c_1 f_i''' + c_2 f_i'' + c_3 f_i' + c_4 f_i + c_5 \theta_i' + c_6 \theta_i = c_7 \tag{21}$$

$$d_1 f_i' + d_2 f_i + d_3 \theta_i'' + d_4 \theta_i' + d_5 \theta_i = d_6 \tag{22}$$

where:

$a_1 = c_1 = (1 + A) - A(\sum_{m=0}^{i-1} \theta_m),\ \ a_2 = \frac{7}{4}\sum_{m=0}^{i-1} f_m - A\sum_{m=}^{i-1} \theta_m{}',$

$a_3 = -\sum_{m=0}^{i-1} f_m{}',\ \ a_4 = \frac{7}{4}\sum f_m'',\ \ a_5 = c_5 = -A\sum_{m=0}^{i-1} f_m{}'',$

$a_6 = c_6 = 1 - A(\sum_{m=0}^{i-1} f_m{}'')$,

$a_7 = \left(-(1+A) + A\sum_{m=0}^{i-1}\theta_m\right)f_m''' + \left(A\sum_{m=0}^{i-1}\theta_m' - \frac{7}{4}\sum_{m=0}^{i-1} f_m\right)f_m'' + \frac{1}{2}\left(\sum_{m=0}^{i-1} f_m'\right)^2 - \theta_m$,

$b_1 = \frac{7}{4}\sum_{m=0}^{i-1}\theta_m'$, $b_2 = d_3 = \frac{1}{\mathrm{Pr}} + \frac{\in}{\mathrm{Pr}}\sum_{m=0}^{i-1}\theta_m$, $b_3 = \frac{2\in}{\mathrm{Pr}}\sum_{m=0}^{i-1}\theta_m' + \frac{7}{4}\sum_{m=0}^{i-1} f_m$,

$b_4 = \frac{\in}{\mathrm{Pr}}\sum_{m=0}^{i-1}\theta_m'$,

$b_5 = \left(-\frac{1}{\mathrm{Pr}} - \frac{\in}{\mathrm{Pr}}(\sum_{m=0}^{i-1}\theta_m)\right)\sum_{m=0}^{i-1}\theta_m{}'' - \frac{\in}{\mathrm{Pr}}\left(\sum_{m=0}^{i-1}\theta_m'\right)^2 - \frac{7}{4}\left(\sum_{m=0}^{i-1} f_m\right)\left(\sum_{m=0}^{i-1}\theta_m'\right)$,

$c_2 = \frac{9}{5}\sum f_m - A\sum\theta_m'$, $c_3 = -\frac{6}{5}\sum f_m'$, $c_4 = \frac{9}{5}\sum f_m''$,

$c_7 = -(1+A)\sum f_m''' - \frac{9}{5}\sum f_m\sum f_m'' + \frac{3}{5}\sum(f_m')^2 + A\theta_m'\sum f_m'' + A\sum\theta_m\sum f_m'' - \sum\theta_m$,

$d_1 = -\frac{1}{5}\theta_m$, $d_2 = \frac{9}{5}\theta_m'$, $d_4 = \frac{2\in}{\mathrm{Pr}}\sum\theta_m' + \frac{9}{5}\sum f_m$, $d_5 = \frac{\in}{\mathrm{Pr}}\sum\theta_m'' - \frac{1}{5}\sum f_m'$,

$d_6 = -\frac{1}{\mathrm{Pr}}\sum\theta_m'' - \frac{\in}{\mathrm{Pr}}\sum\theta_m\sum\theta_m'' - \frac{\in}{\mathrm{Pr}}(\sum\theta_m')^2 + \frac{1}{5}\sum\theta_m\sum f_m' - \frac{9}{5}\sum f_m\sum\theta_m'$

The solution to the linearized Equations (19)-(22) is achieved by means of the Chebyshev collocation method which is constructed on the Chebyshev polynomials. In this problem, the domain of the solution $[0, \infty)$ is transformed to $[0, L]$, where L is a constant utilized to acquire the ambient boundary conditions. To apply this method, $[0, L]$ is again changed to $[-1, 1]$ by using the mapping

$$\frac{\eta}{L} = \frac{\xi+1}{2},\ -1 \le \xi \le 1. \tag{23}$$

The functions f_i and θ_i are guesstimated at the following grid points due to Gauss--Lobatto

$$\xi_j = \cos\frac{\pi j}{N},\ j = 0,1,2,3 \ldots N \tag{24}$$

as

$$f_i(\xi) = \sum_{k=0}^{N} f_i(\xi_K)T_k(\xi_j),\ \theta_i(\xi) = \sum_{k=0}^{N}\theta_i(\xi_k)T_k(\xi_j),\ j = 0,1,2 \ldots N \tag{25}$$

where $T_k(\xi) = \cos[k\cos^{-1}(\xi)]$ is the k^{th} degree Chebyshev polynomial.

r^{th} derivative of f_i and θ_i are approximated

$$\frac{d^r f_i}{d\eta^r} = \sum_{k=0}^{N} D_{kj}^r f_i(\xi_k),\ \frac{d^r\theta_i}{d\eta^r} = \sum_{k=0}^{N} D_{kj}^r\theta_i(\xi_k),\ j = 0,1,2 \ldots N \tag{26}$$

where $D = \frac{2}{L}D$ with D is the Chebyshev spectral differentiation matrix.

Substitution of Eqs. (26)-(27) into equations (19)-(20) and (21)-(22) gives the equation in matrix form as

$$A_{i-1}X_i = R_{i-1} \tag{27}$$

where A_{i-1} is a square matrix of order 2N + 2 and X_i and R_{i-1} are column matrices of order 2N + 2 given by

$$A_{i-1} = \begin{bmatrix} A_{11}^{(i)} & A_{12}^{(i)} \\ A_{21}^{(i)} & A_{22}^{(i)} \end{bmatrix}, X_i = \begin{bmatrix} F_i \\ \Theta_i \end{bmatrix}, \; R_{i-1} = \begin{bmatrix} r_1^{(i)} \\ r_2^{(i)} \end{bmatrix}. \tag{28}$$

where:

$F_i = [f_i(\xi_0), f_i(\xi_1), .., f_i(\xi_N)]^T, \;\; \Theta_i = [\theta_i(\xi_0), \theta_i(\xi_1), .., \theta_i(\xi_N)]^T,$
$A_{11}^{(1)} = a_1 D^3 + a_2 D^2 + a_3 D + a_4 I, \;\; A_{12}^{(1)} = a_5 D + a_6 I, \;\; A_{21}^{(1)} = b_1 I,$
$A_{22}^{(1)} = b_2 D^2 + b_3 D + b_4 I, \;\; r_1^{(1)} = [a_7(\xi_0), a_7(\xi_1), \ldots, a_7(\xi_{N-1}), a_7(\xi_N)]^T,$
$r_2^{(1)} = [b_5(\xi_0), b_5(\xi_1), \ldots, b_5(\xi_{N-1}), b_5(\xi_N)]^T, \; A_{11}^{(2)} = c_1 D^3 + c_2 D^2 + c_3 D + c_4 I,$
$A_{12}^{(2)} = c_5 D + c_6 I, \;\; A_{21}^{(2)} = d_1 D + d_2 I, \;\; A_{22}^{(2)} = d_3 D^2 + d_4 D + d_5 I,$
$r_1^{(2)} = [c_7(\xi_0), c_7(\xi_1), .., c_7(\xi_{N-1}), c_7(\xi_N)]^T,$
$r_2^{(2)} = [d_6(\xi_0), d_6(\xi_1), .., d_6(\xi_{N-1}), d_6(\xi_N)]^T$ (29)

where the superscript T stands for transpose, I is the identity, and 0 is the zero matrices. Finally, the solution is given by

$$X_i = A_{i-1}^{-1} R_{i-1} \tag{30}$$

4. Results and discussion

The present study computes the velocity component f', the temperature θ, local Nusselt number N_u, and the coefficient of local skin friction C_f for diverse values of viscosity parameter A, and thermal conductivity parameter $\in$ for the cases of wall temperature and heat flux and depicts graphically.

The impact of viscosity parameter A on the velocity component, temperature, coefficient of skin friction, and the heat transfer rate is depicted in Figure 2 for type – I boundary conditions. It is detected from Figure 2a that the velocity rises near the cone, reaches its peak value, and then declines gradually to zero as $\eta \to \infty$. Furthermore, it is perceived that as the value of A intensifies, the velocity reduces adjacent to the cone and enhances away from the cone. The temperature increases slightly for an increase in A as portrayed in Figure 2b. As shown in Figure 2c, increasing A raises the skin friction coefficient. The rate of heat transfer declines as A escalates as presented in Figure 2d.

The variation of f', θ, C_f and N_u with the thermal conductivity, parameter $\in$ is given in Figure 3 for type – I boundary conditions. Figures 3a and 3b exhibit that as the value of $\in$ grows, so do the velocity f' and the temperature θ. The coefficient of skin friction is increasing, whereas the rate of heat transfer is decreasing for rising values of $\in$ as shown in Figures 3c and 3d.

Figure 4 presents the influence of viscosity parameter A on the velocity component, temperature, coefficient of skin friction, and heat transfer rate for type – II boundary conditions. The impact of the viscosity parameter is less significant in comparison to the type – I boundary conditions, as seen in Figure 4. For increasing

values of A, the velocity enhances adjacent to the cone and decays away from the cone. The temperature is also decreasing for increasing values of A as revealed in Figure 4b. As seen in Figure 4c, increasing A slightly enhances the skin friction coefficient. As A increases, so does the heat transfer rate as presented in Figure 4d.

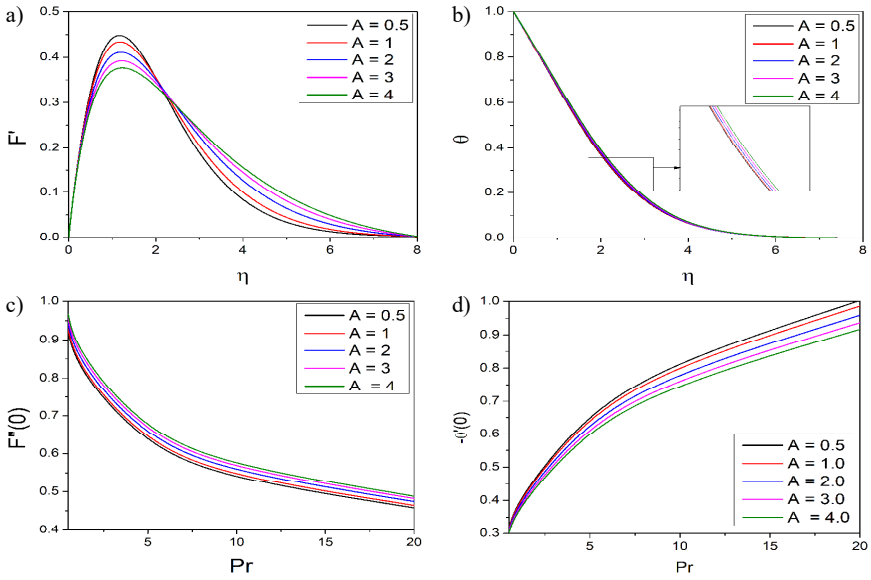

Fig. 2. Effect of A on: a) velocity, b) temperature, c) skin friction coefficient and d) Nusselt number for CWT boundary conditions

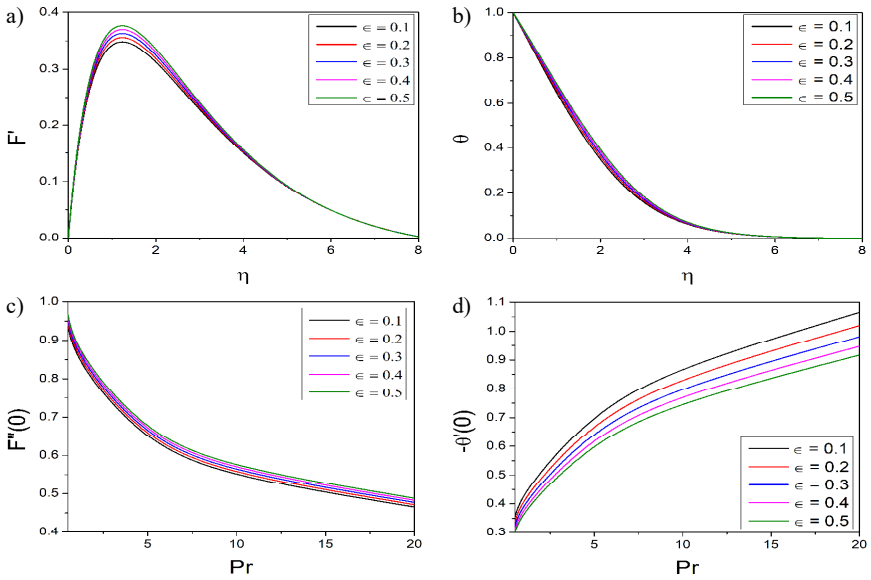

Fig. 3. Effect of $\in$: a) velocity, b) temperature, c) skin friction coefficient and d) Nusselt number for CWT boundary conditions

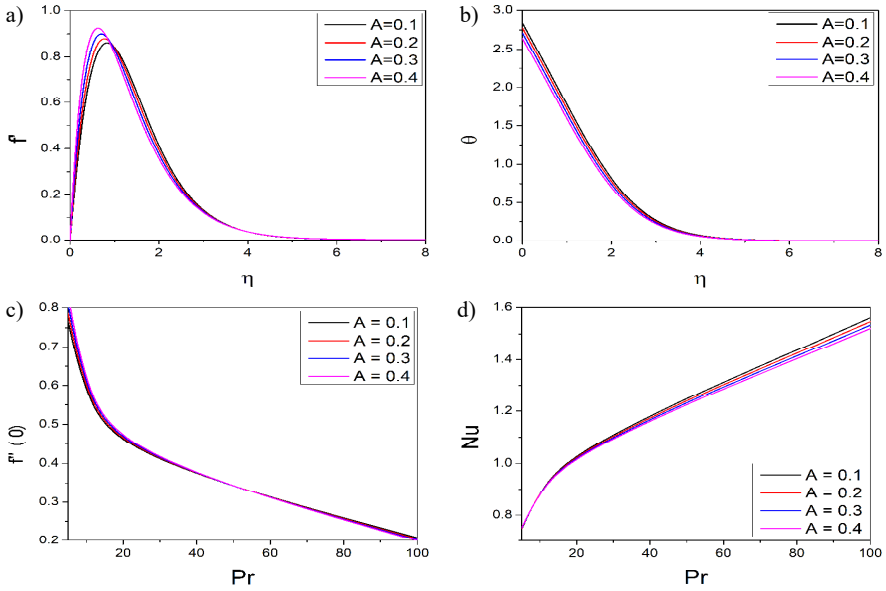

Fig. 4. Effect of A on: a) velocity, b) temperature, c) skin friction coefficient and d) Nusselt number for CHF boundary conditions

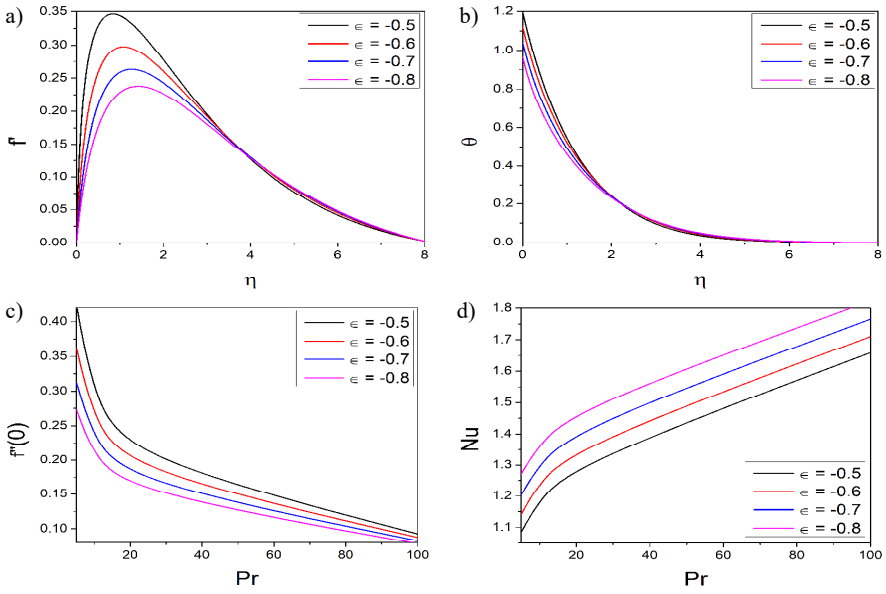

Fig. 5. Effect of ∈: a) velocity, b) temperature, c) skin friction coefficient and d) Nusselt number for CHF boundary conditions

The variation of the velocity component, temperature, coefficient of skin friction, and Nusselt number with the thermal conductivity parameter ∈, is shown in Figure 5 for type – II boundary conditions. According to Figure 5a, velocity declines with

enhancing the thermal conductivity parameter. Figure 5b reveals that the effect of $\in$ on the temperature is not very significant. The skin friction coefficient is decreasing, whereas the Nusselt number is escalating for increasing values of $\in$ as shown in Figures 5c and 5d.

5. Conclusion

The free convection flow across a vertical cone is investigated under the supposition that viscosity and thermal conductivity change with temperature. Similarity transformation is utilized to convert the equations administering the flow into ordinary differential equations. The non-dimensional equations are linearized by employing a successive linearization procedure, and then the solution of the consequent system is found using the Chebyshev spectral method.

- If the viscosity parameter is enhanced, the velocity adjacent to the cone surface increases, while the reverse tendency is observed sufficiently away from the cone surface.
- The local heat transfer rate decreases with increasing the viscosity and thermal conductivity parameters for CWT conditions, but the reverse trend is noticed for CHF conditions.
- For the CWT state, an increase in viscosity and thermal conductivity parameters infers a rise in the coefficient of the skin friction, whereas, for CWF conditions, the opposite is the case.

References

[1] Merk, H.J., & Prins, J.A. (1954). Thermal convection in laminar boundary layers II. *Applied Scientific Research*, *4*(3), 195-206.

[2] Hering, R., & Grosh, R. (1962). Laminar free convection from a non-isothermal cone. *International Journal of Heat and Mass Transfer*, *5*(11), 1059-1068.

[3] Kafoussias, N. (1992). Effects of mass transfer on free convective flow past a vertical isothermal cone surface. *International Journal of Engineering Science*, *30*(3), 273-281.

[4] Ece, M.C. (2005). Free convection flow about a cone under mixed thermal boundary conditions and a magnetic field. *Applied Mathematical Modelling*, *29*(11), 1121-1134.

[5] Palani, G., & Ragavan, A.R. (2015). Free convection flow past a vertical cone with a chemical reaction in the presence of transverse magnetic field. *Journal of Engineering Physics and Thermophysics*, *88*(5), 1256-1263.

[6] Vanita, & Kumar, A. (2016). Numerical study of effect of induced magnetic field on transient natural convection over a vertical cone. *Alexandria Engineering Journal*, *55*(2), 1211-1223.

[7] Ajay, C.K., & Srinivasa, A.H. (2020). Unsteady MHD natural convective boundary layer flow and heat transfer over a truncated cone in the presence of pressure work. *Journal of Applied Mathematics and Computational Mechanics*, *19*(1), 5-16.

[8] Kannan, R.M., Pullepu, B., & Sajid, M. (2022). Free convective flow past a vertical cone with magnetohydrodynamics / heat generation / absorption with Variable heat flux. *Mathematical Modelling of Engineering Problems*, *9*(1), 11-18.

[9] Kays, W.M., & Crawford, M.E. (1980). *Convective Heat and Mass Transfer*. McGraw-Hill Companies.

[10] Herwig, H., & Wickern, G. (1986). The effect of variable properties on laminar boundary layer flow. *Wärme- und Stoffübertragung*, *20*(1), 47-57.

[11] Chand, R., Rana, G.C., & Kumar, S.. (2013). Variable gravity effects on thermal instability of nanofluid in anisotropic porous medium. *International Journal of Applied Mechanics and Engineering*, *18*(3), 631-642.

[12] Choudhury, M., & Hazarika, G. (2013). The effects of variable viscosity and thermal conductivity on MHD oscillatory free convective flow past a vertical plate in slip flow regime with variable suction and periodic plate temperature. *Journal of Applied Fluid Mechanics*, *6*(2), 277-283.

[13] Mekheimer, K.S., & Abd Elmaboud, Y. (2014). Simultaneous effects of variable viscosity and thermal conductivity on peristaltic flow in a vertical asymmetric channel. *Canadian Journal of Physics*, *92*(12), 1541-1555.

[14] Anjali Devi, S.P., & Prakash, M. (2015). Temperature dependent viscosity and thermal conductivity effects on hydromagnetic flow over a slendering stretching sheet. *Journal of the Nigerian Mathematical Society*, *34*(3), 318-330.

[15] Umavathi, J.C., Chamkha, A.J., & Mohiuddin, S. (2016). Combined effect of variable viscosity and thermal conductivity on free convection flow of a viscous fluid in a vertical channel. *International Journal of Numerical Methods for Heat & Fluid Flow*, *26*(1), 18-39.

[16] Srinivasacharya, D, & Jagadeeshwar, P. (2018). Effect of variable properties on the flow over an exponentially stretching sheet with convective thermal conditions. *Modelling, Measurement and Control B*, *87*(1), 7-14.

[17] Mushtaq, A., Farooq, M.A., Sharif, R., & Razzaq, M. (2019). The impact of variable fluid properties on hydromagnetic boundary layer and heat transfer flows over an exponentially stretching sheet. *Journal of Physics Communications*, *3*(9), 095005.

[18] Ahmed, S., Hazarika, G.C., & Gogoi, G. (2020). Investigation of variable viscosity and thermal conductivity on MHD mass transfer flow problem over a moving non-isothermal vertical plate. *Journal of Naval Architecture and Marine Engineering*, *17*(2), 183-197.

[19] Ahmad, U., Ashraf, M., Al-Zubaidi, A., Ali, A., & Saleem, S. (2021). Effects of temperature dependent viscosity and thermal conductivity on natural convection flow along a curved surface in the presence of exothermic catalytic chemical reaction. *PLOS ONE*, *16*(7), e0252485.

[20] Chu, Y.M., Shah, F., Khan, M. I., Kadry, S., Abdelmalek, Z., & Khan, W.A. (2020). Cattaneo--Christov double diffusions (CCDD) in entropy optimized magnetized second grade nanofluid with variable thermal conductivity and mass diffusivity. *Journal of Materials Research and Technology*, *9*(6), 13977-13987.

[21] Khan, M.I., Khan, S.U., Jameel, M., Chu, Y.M., Tlili, I., & Kadry S. (2021). Significance of temperature-dependent viscosity and thermal conductivity of Walter's B nanoliquid when sinusoidal wall and motile microorganisms' density are significant. *Surfaces and Interfaces*, *22*, 100849.

[22] Song, Y.Q., Waqas, H., Al-Khaled, K., Farooq, U., Khan, S.U., Khan, M.I., Chu, Y.M., & Qayyum, S. (2021). Bioconvection analysis for Sutterby nanofluid over an axially stretched cylinder with melting heat transfer and variable thermal features: A Marangoni and solutal model. *Alexandria Engineering Journal*, *60*(5), 4663-4675.

[23] Salahuddin, T., Khan, M., Saeed, T., Ibrahim, M., & Chu, Y.M. (2021). Induced MHD impact on exponentially varying viscosity of Williamson fluid flow with variable conductivity and diffusivity. *Case Studies in Thermal Engineering*, *25*, 100895.

[24] Islam, T., Alam, M.N., Asjad, M.I., Praveen, N., & Chu, Y.M. (2021). Heatline visualization of MHD natural convection heat transfer of nanofluid in a prismatic enclosure. *Scientific Reports*, 11, 10972.

[25] Sarker, S.P.K., & Alam, M.M. (2021). Effect of variable viscosity and thermal conductivity on MHD natural convection flow along a vertical flat plate. *Journal of Advances in Mathematics and Computer Science*, *36*(3), 58-71.

[26] Hasan, M.F., Molla, M.M., Kamrujjaman, M., & Siddiqa, S. (2022). Natural convection flow over a vertical permeable circular cone with uniform surface heat flux in temperature-dependent viscosity with three-fold solutions within the boundary layer. *Computation*, *10*(4), 60.